JOURNAL OF APPLIED ELECTROCHEMISTRY **28** (1998) 1365–1369

Electrochemical evaluation of $LiCoO_2$ synthesized by decomposition and intercalation of hydroxides for lithium-ion battery applications

B. HUANG, Y-I. JANG, Y-M. CHIANG, D. R. SADOWAY*

Department of Materials Science and Engineering, Massachusetts Institute of Technology,
Cambridge, MA 02139-4307, USA

Received 13 March 1998; accepted in revised form 19 May 1998

$LiCoO_2$ has been synthesized by a solid-state synthesis route involving the decomposition and intercalation of hydroxide precursors generated by precipitation and freeze-drying. Cyclic voltammetry of $LiCoO_2$ obtained by heating at 100 °C for 2 h has shown this material to be electrochemically active with an initial discharge capacity of $92\,\mathrm{mA\,h\,g^{-1}}$. Optimization of processing conditions reduced the firing time to as little as 2 h at 800 °C, producing $LiCoO_2$ powders with high reversible capacity ($142\,\mathrm{mA\,h\,g^{-1}}$), good rate capability, and good cyclability. The favourable performance of this oxide powder in $LiCoO_2$/C lithium-ion cells using the present oxide powders shows the instant synthesis route to be promising and cost-effective for lithium-ion battery applications.

Keywords: *cathode*, *cyclic voltammetry*, *intercalation/deintercalation*, *$LiCoO_2$*, *lithium-ion battery*

---

1. Introduction

Extensive studies have been conducted on $LiCoO_2$ having the α-$NaFeO_2$ structure type as a cathode material for lithium-ion batteries [1–3]. Although $LiCoO_2$ is costly, it possesses certain attributes such as ease of preparation and elevated temperature utility, and hence is favoured over cheaper competitors like $LiNiO_2$ and $LiMn_2O_4$ in commercial lithium-ion battery manufacturing [4–6]. Synthesis of $LiCoO_2$ is typically carried out by a solid-state reaction process involving mechanical mixing of lithium salts and cobalt compounds followed by firing at high temperatures and intermittent grindings, sometimes extended firing for over 24 h at 800–1000 °C [7]. The conditions for making high-performance oxide material (called HT-$LiCoO_2$) rely upon long-range diffusion of reactants and hence may result in poor control of chemical homogeneity as well as high cost for heat treatment. Many attempts have been made to synthesize this compound by solution methods at lower temperatures and/or for a shorter reaction time [4, 8–12]. Although Garcia *et al.* [9, 10, 12] were able to make electrochemically active $LiCoO_2$ by firing precipitated precursors at 800 °C for 2 h, they were not successful in the synthesis of $LiCoO_2$ having the α-$NaFeO_2$ structure type at temperatures as low as 400 °C. Instead, they obtained an oxide with disordered structure, referred to as LT-$LiCoO_2$. Under hydrothermal conditions, Amatucci *et al.* [4, 11] synthesized $LiCoO_2$ of the α-$NaFeO_2$ structure-type at 100 °C with the reaction time longer than 2–3 days, but they still had to heat-treat the compound at high temperature to improve the electrochemical performance.

In a previous paper [13], we reported a new solid-state reaction method that can produce $LiCoO_2$ of the α-$NaFeO_2$ structure type at low temperatures with short reaction times. The mechanism of transformation was determined using transmission electron microscopy and X-ray diffraction. Decomposition of $Co(OH)_2$ and intercalation of lithium cause the homogeneous precursor obtained by precipitation and freeze-drying to transform directly to HT-$LiCoO_2$ upon heating in air at temperatures of 200–300 °C for 2 h. From preliminary electrochemical tests, we showed that the product obtained at 100 °C is electrochemically active, and firing at high temperatures further improves capacity and cyclability. In this paper, we provide more information on the electrochemical properties of $LiCoO_2$ obtained by this new synthesis route. Cyclic voltammetry and galvanostatic charge-discharge studies have been performed to investigate the electrochemical properties of materials obtained at various temperatures. These oxide powders have also been tested as the cathode-active material in lithium-ion batteries comprising graphite anode and liquid electrolyte.

2. Experimental details

$LiCoO_2$ powders were synthesized by decomposition and intercalation of hydroxide precursors, as described previously [13]. $LiOH.H_2O$ (Alfa Aesar, 98%) and $Co(NO_3)_2.6H_2O$ (Alfa Aesar, 99.5%) were used to prepare the precursors. $Co(OH)_2$ was precipitated

---

* Authors to whom correspondence should be addressed.

0021-891X © 1998 Chapman & Hall

by adding a solution of $Co(NO_3)_2$ to a solution LiOH. The precipitate was purified of nitrate ion species, which otherwise reform low-melting metal nitrates upon firing, by a rinsing procedure described elsewhere [13]. The precipitate was then dispersed in an aqueous solution of LiOH yielding the total composition of 1.05 : 1 in Li : Co on a molar basis. The slight excess of lithium was included to compensate for loss during firing. The suspension was atomized into liquid nitrogen, and the frozen droplets were freeze-dried (VirTis Consol 12LL, Gardiner, NY). The precursor powders thus obtained were fired in air for 2 h at various temperatures between 100 and 800 °C. Calcined powders were characterized by X-ray diffraction (XRD) using a Rigaku diffractometer (RTP500RC) with CuK_α radiation.

For electrochemical evaluation, cathodes were prepared by mixing together the $LiCoO_2$ powders, carbon black (Cabot), and poly(vinylidene fluoride) (PVDF) (Aldrich) in the weight ratio of 78:12:10. PVDF was pre-dissolved in γ-butyrolactone (Aldrich) before mixing with the other components. After the γ-butyrolactone was evaporated at 150 °C in air, the components were compacted at about $4\,t\,cm^{-2}$ pressure to form pellets 10–25 mg in weight and $0.5\,cm^2$ in cross-sectional area. The pellets were then dried at 140 °C under primary vacuum for 24 h and transferred to an argon-filled glove box.

In this study two kinds of cell were employed for battery testing: lithium and lithium-ion. In lithium cells, the anode consisted of lithium ribbon of 0.75 mm thickness (Aldrich), while in lithium-ion cells the anode consisted of graphite (Timcal America). The latter was prepared by spreading graphite slurries onto a stainless steel screen substrate followed by drying and compacting. The slurry contained graphite, PVDF in γ-butyrolactone solvent. The composition of the slurry was adjusted so that about 10% of the finished electrode mass was PVDF and about 90% of the finished electrode mass was graphite. After γ-butyrolactone was evaporated at 150 °C in air, electrode were compacted at about $4\,t\,cm^{-2}$ pressure between flat plates and then cut into squares measuring 1 cm × 1 cm. The typical electrode thickness was about 0.2 mm. The separator was a film of Celgard 2400^{TM}, and the electrolyte consisted of a 1 M solution of $LiPF_6$ in ethylene carbonate (EC) and diethyl carbonate (DEC) (EM Industries). The ratio of EC to DEC was 1:1 by volume. All cell handling was performed in an argon-filled glove box.

Cyclic voltammetry was performed in a three-electrode cell with a Solartron 1286 potentiostat controlled by CorrWare running on an IBM PC. Data were taken at a scan rate of $v = 0.01\,mV\,s^{-1}$ over the potential range in which no electrolytic decomposition occurs. The $LiCoO_2$ working electrode, $0.2\,cm^2$ in cross-sectional area, was prepared in the same manner described above for preparation of the battery cathode. Lithium foil, $2\,cm^2$ in cross-sectional area, served as the counter electrode, and lithium wire served as the reference electrode. Charge–discharge studies on lithium cells and lithium-ion cells were performed with a battery tester (MACCOR Automated Test System, series 4000) at various current densities with the voltage limit between 2.5 and 4.25 V.

3. Results and discussion

Figure 1(a) shows the cyclic voltammogram of $LiCoO_2$ fired at 100 °C for 2 h. One can observe three peaks in the anodic scan. The main peak appears at 3.98 V. There is also a broad peak at 3.70 V. These oxidation peaks, including a small peak at 4.15 V, correspond to the extraction of Li^+ ions from the $LiCoO_2$ host. During the cathodic scan, the main reduction peak appears at 3.84 V, and a small peak can be found at 3.65 V. These results indicate that the powder obtained at 100 °C in this study is electrochemically active. However, the oxide is predominantly LT-$LiCoO_2$ as seen in the XRD pattern in Fig. 2. It is well-known that the presence of the well-ordered HT-$LiCoO_2$ is evidenced by splitting of the (006)/(012) peaks and (108)/(110) peaks [7] (Fig. 2), something not seen in the spectrum of the oxide fired at 100 °C. Although the decomposition of hydroxides and the intercalation of lithium begin to occur at around 100 °C, the resulting $LiCoO_2$ does not exhibit perfect α-$NaFeO_2$ structure-type cation ordering at this temperature. Interestingly, however, comparison with previous cyclic voltammetry on LT- and HT-$LiCoO_2$ [10, 12, 14] indicates that the present material begins to exhibit characteristics of HT-$LiCoO_2$. According to Garcia *et al.* [10, 12], LT-$LiCoO_2$ obtained at 400 °C is characterized by broad anodic and cathodic peaks separated by a potential difference exceeding 0.3 V. Peaks were reported to be located at 3.75 and 3.45 V during the anodic and cathodic scans, respectively. Gummow *et al.* [14] also observed 4 and 3.2 V main peaks during anodic and cathodic scans, respectively, with a potential difference exceeding 0.8 V from their LT-$LiCoO_2$ prepared at 400 °C. In addition to the 3.2 V reduction peak, they also observed a minor peak at 3.7 V. As shown in Fig. 1(a), the present oxide has a voltammoagram similar in shape to that of HT-$LiCoO_2$ in terms of the potential difference (0.14 V) between main peaks during anodic and cathodic scans. Furthermore, we have a higher reduction peak at 3.85 V than at 3.65 V, which supports the existence of significant HT-$LiCoO_2$ after firing at only 100 °C.

Fig. 3(a) shows charge–discharge curves for the present material fired at 100 °C for 2 h. Lithium cells were cycled at room temperature between 2.5 and 4.25 V at a current density of $0.4\,mA\,cm^{-2}$ (corresponding to the $0.2\,C$ rate). $LiCoO_2$ has an initial discharge capacity as high as $92\,mA\,h\,g^{-1}$. This confirms that the material is electrochemically active.

To our knowledge, the present synthesis method has the distinction of requiring the lowest temperature and shortest heat treatment time ever reported for $LiCoO_2$. Although there have been previous re-

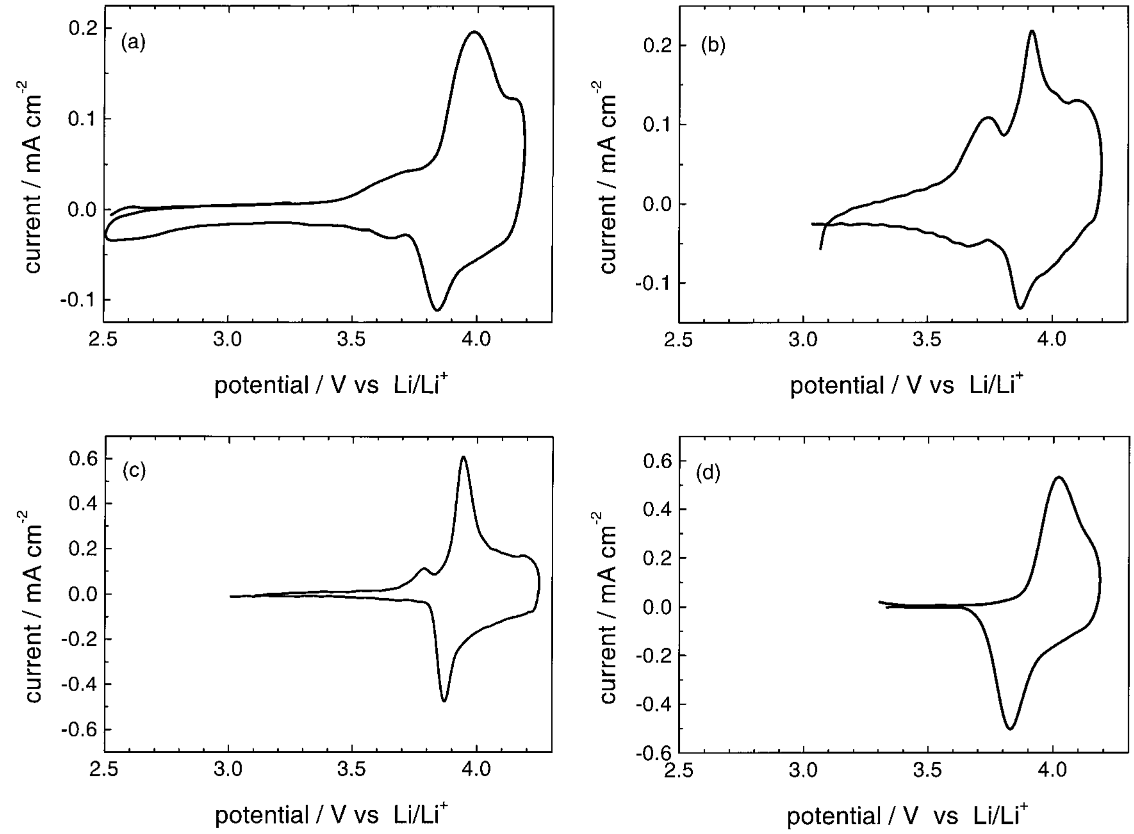

Fig. 1. Cyclic voltammograms of $LiCoO_2$ fired for 2 h at various temperatures: (a) 100, (b) 300, (c) 600 and (d) 800 °C. Scan rate 0.01 mV s^{-1}.

ports that $LiCoO_2$ can be obtained at 100°C by cationic exchange reaction under hydrothermal conditions [4, 11], Larcher *et al.* [4] observed that the reaction requires two days for completion, far exceeding the heat treatment times employed in this study. Even so, it must be conceded that, as discussed elsewhere [13], material calcined at such a low temperature as 100 °C does not exhibit good cyclability. In Fig. 3(a), fast capacity fade upon cycling can be clearly seen.

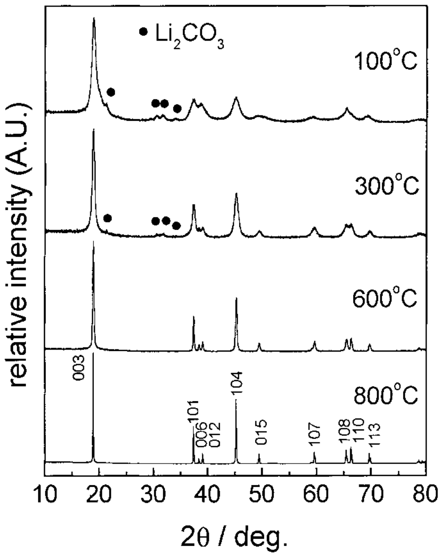

Fig. 2. X-ray diffraction patterns of $LiCoO_2$ fired for 2 h at various temperatures: (a) 100, (b) 300, (c) 600 and (d) 800 °C (with *hkl* indexed for a hexagonal setting, (●): Li_2CO_3).

As shown in Fig. 2, crystallinity and cation ordering in the α-$NaFeO_2$ structure-type increases with firing temperature. The extra peaks in the specimens fired at low temperatures (i.e., at 100 °C and 300 °C) match those of lithium carbonate. Therefore, as the firing temperature increases, one can expect better-defined anodic and cathodic main peaks and reduced minor peaks. This is precisely what we observed in this study. Fig. 1(b) shows the results for $LiCoO_2$ fired at 300 °C. Although the broad minor peaks still appear, the main anodic and cathodic peaks at 3.92 and 3.87 V are better defined than those in Fig. 1(a). Figure 1(c) shows the results for $LiCoO_2$ fired at 600 °C. Well defined anodic and cathodic peaks at 3.94 and 3.87 V, respectively, are evident as well as reduced minor peaks compared with Fig. 1(b). Cyclic voltammetry of $LiCoO_2$ fired at 800 °C is shown in Fig, 1(d) in the scan range between 3.3 and 4.25 V. Two distinct current peaks at 4.01 and 3.84 V are observed. No minor peaks were observed during either the anodic or the cathodic scan. This indicates that $LiCoO_2$ fired at 800 °C has a well-ordered α-$NaFeO_2$ structure. It is also worth noting in Fig. 1 that reversibility increases with firing temperature. While the areas under the *i*/*V* curves for cathodic scans are much less than those for anodic scans for samples fired at low temperatures, the difference in areas decreases with firing temperature, indicating that the reversibility of the present material improves

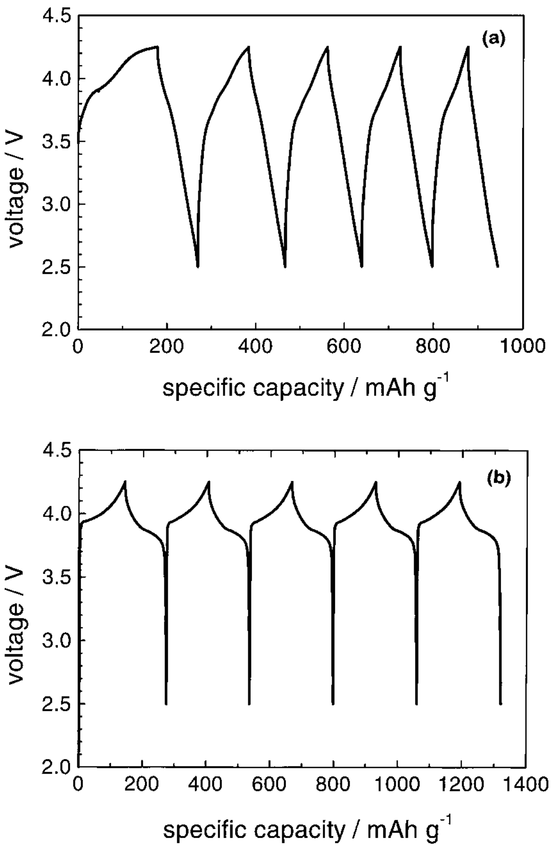

Fig. 3. Charge–discharge curves of $LiCoO_2$/Li cells using $LiCoO_2$ fired for 2 h at various temperatures: (a) 100 and (b) 800 °C. Voltage range 2.5 to 4.25 V. Current density 0.4 mA cm^{-2} (corresponding to the 0.2 *C* rate).

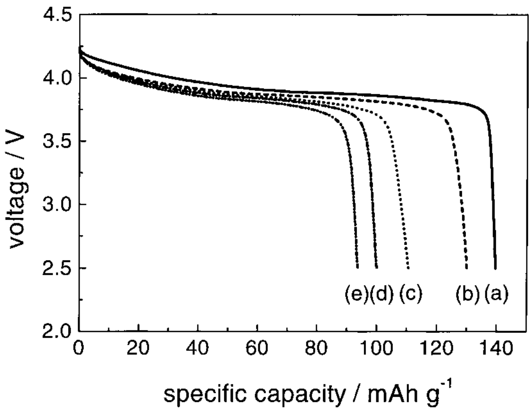

Fig. 4. Effect of current density on the specific capacity of $LiCoO_2$ fired at 800 °C. Equal charge and discharge currents were employed when the cells were discharged at (a) 0.4 mA cm^{-2} (corresponding to the 0.2 *C* rate) and (b) 0.8 mA cm^{-2} (corresponding to the 0.4 *C* rate). When the cells were discharged at (c) 1.2 mA cm^{-2} (corresponding to the 0.6 *C* rate). (d) 1.6 mA cm^{-2} (corresponding to the 0.8 *C* rate) and (e) 2.0 mA cm^{-2} (corresponding to the 1 *C* rate), a charging current of 0.4 mA cm^{-2} (corresponding to the 0.2 *C* rate) was imposed.

with firing temperature. It is easier to appreciate that when the areas under *i*/*V* anodic and cathodic curves are nearly identical, the coulombic efficiency Q_c/Q_a is high, evidence of good reversibility for the intercalation–deintercalation reaction. On this basis, we compute coulombic efficiencies of about 60% and about 95% for oxides fired at 100 °C and 800 °C, respectively.

Figure 3(b) shows charge-discharge curves for a lithium cell cycled at a current density of 0.4 mA cm^{-2} (corresponding to the 0.2 *C* rate) between 2.5 and 4.25 V. The cathode contained $LiCoO_2$ fired at 800 °C. The cell exhibited good cyclability and high capacity (142 mA h g^{-1}). Figure 4 shows the results of tests carried out at various current densities. It is evident that the present material has good rate capability, delivering 92 mA h g^{-1} at 2 mA cm^{-2} (corresponding to the 1 *C* rate) and keeping over 70% of its capacity at 0.4 mA cm^{-2}.

Lithium-ion cells using graphite anode were fabricated using $LiCoO_2$ powder fired at 800 °C as the cathode active material. One of the problems of carbon anodes in C/Li cells is irreversible capacity loss (>20%) during the first discharge or first lithiation [15, 16]. It is generally recognized that the irreversible capacity loss arises from electrolyte decomposition followed by the formation of a passivation layer or solid–electrolyte interface (SEI) on the carbon surface [16]. To address this problem, here the graphite had been pretreated before introduction into the Li-ion cells. Figure 5 shows the voltage profiles of graphite/Li cells as a function of capacity during the first discharge/charge at room temperature between 0.01 and 2.0 V at a current density of 0.4 mA cm^{-2}. As shown in Fig. 5(a), cells using untreated graphite have a first discharge capacity of 430 mA h g^{-1} when discharged to 0.01 V, and a first charge capacity of

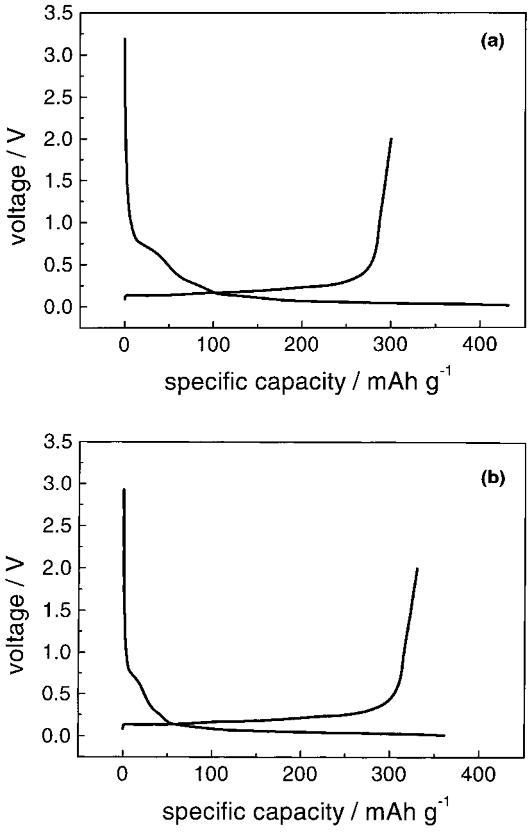

Fig. 5. Charge–discharge curves of C/Li cell between 0.01 and 2.0 V at a current density of 0.4 mA cm^{-2} using (a) untreated graphite and (b) pretreated graphite as anode.

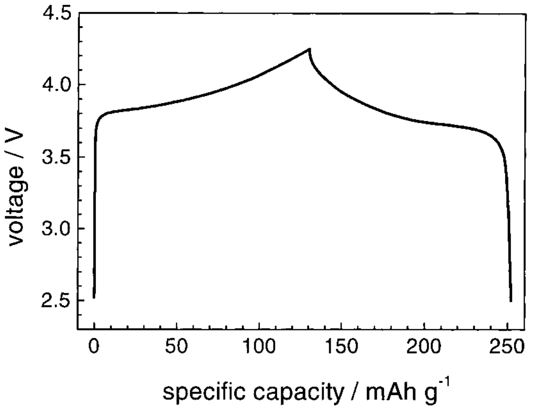

Fig. 6. Typical charge–discharge curve of $LiCoO_2$/C cell between 2.5 and 4.25 V at a current density of 0.4 mA cm^{-2} (corresponding to the 0.2 *C* rate).

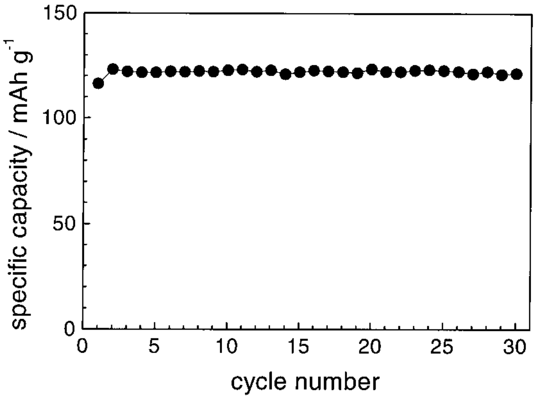

Fig. 7. Specific capacity vs. cycle number for a $LiCoO_2$/C cell between 2.5 and 4.25 V at a current density of 0.4 mA cm^{-2} (corresponding to the 0.2 *C* rate).

300 mA h g^{-1} based on the weight of graphite. The capacity loss during the first cycle is 130 mA h g^{-1}, corresponding to 30% loss. However, the pretreated graphite has an 8% irreversible capacity loss as shown in Fig. 5(b) with first discharge capacity of 361 mA h g^{-1} and first charge capacity of 332 mA h g^{-1}.

Figure 6 shows a typical charge-discharge curve of a $LiCoO_2$/C cell at room temperature between 2.5 and 4.25 V at a constant current density of 0.4 mA cm^{-2} (corresponding to the 0.2 *C* rate). The cell delivers a reversible capacity of 120 mA h g^{-1} based on the weight of the cathode-active oxide. Because the voltage of the graphite electrode is relatively flat, one can clearly observe the charge/discharge plateaus around 4 V. Evidence of the excellent cyclability of this cell is provided in Fig. 7 which shows the capacity against cycle number. These results demonstrate that $LiCoO_2$ prepared by the present synthesis route possesses high capacity and exhibits good cyclability and hence is useful as a cathode material for lithium-ion batteries.

4. Conclusion

$LiCoO_2$ has been synthesized by a new solid state reaction method incorporating precipitation and freeze-drying of hydroxide precursors. Electrochemical properties of the present material were studied as a cathode material for rechargeable lithium batteries and lithium-ion batteries. Results show that the powder obtained at temperatures as low as 100 °C is electrochemically active and has characteristics of HT-$LiCoO_2$. Firing at higher temperatures further improves the reversible capacity and cyclability. These results indicate that the current synthesis route is a promising method for preparing $LiCoO_2$ as a cathode material for lithium-ion batteries. This new method may also be useful for other intercalation oxides.

Acknowledgements

We thank Professors G. Ceder and A. M. Mayes for helpful discussions and Dr H. Wang for experimental assistance. This work was supported by Furukawa Electric Company and the Idaho National Engineering and Environmental Laboratory under grant C95-175002, and used instrumentation in the Shared Central Facilities at MIT, supported by NSF grant 9400334-DMR.

References

[1] K. Mizushima, P. C. Jones, P. J. Wiseman and J. B. Goodenough, *Mat. Res. Bull.* **15** (1980) 783.
[2] K. Ozawa, *Solid State Ionics* **69** (1994) 212.
[3] G. G. Amatucci, J. M. Tarascon and L. C. Klein, *ibid.* **83** (1996) 167.
[4] D. Larcher, M. R. Palacin, G. G. Amatucci and J. M. Tarascon, *J. Electrochem. Soc.* **144** (1997) 408.
[5] G. G. Amatucci, A. Blyr, C. Sigala, P. Alfonse and J. M. Tarascon, *Solid State Ionics* **104** (1997) 13.
[6] G. G. Amatucci, C. N. Schmutz, A. Blyr, C. Sigala, A. S. Gozdz, D. Larcher and J. M. Tarascon, *J. Power Sources* **69** (1997) 11.
[7] R. J. Gummow, M. M. Thackeray, W. I. F. David and S. Hull, *Mat. Res. Bull.* **27** (1992) 327.
[8] P. Barboux, J. M. Tarascon and F. K. Shokoohi, *J. Solid State Chem.* **94** (1991) 185.
[9] B. Garcia, P. Barboux, F. Ribot, A. Kahn-Harari, L. Mazerolles and N. Baffier, *Solid State Ionics* **80** (1995) 111.
[10] B. Garcia, J. Farcy, J. P. Pereira-Ramos, J. Perichon and N. Baffier, *J. Power Sources* **54** (1995) 373.
[11] G. G. Amatucci, J. M. Tarascon, D. Larcher and L. C. Klein, *Solid State Ionics* **84** (1996) 169.
[12] B. Garcia, J. Farcy, J. P. Pereira-Ramos and N. Baffier, *J. Electrochem. Soc.* **144** (1997) 1179.
[13] Y.-M. Chiang, Y.-I. Jang, H. Wang, B. Huang, D. R. Sadoway and P. Ye, *ibid.* **145** (1998) 887.
[14] R. J. Gummow, D. C. Liles and M. M. Thackeray, *Mat. Res. Bull.* **28** (1993) 235.
[15] J. M. Tarascon and D. Guyomard, *J. Electrochem. Soc.* **138** (1991) 2864.
[16] W. Xing and J. R. Dahn, *ibid.* **144** (1997) 195.